JOC The Journal of Organic Chemistry

pubs.acs.org/joc Article

Experimental and Computational Study on the Intramolecular Hydrogen Atom Transfer Reactions of Maleimide-Based Enediynes After Cycloaromatization

Mengsi Zhang, Haotian Lu, Baojun Li, Hailong Ma, Wenbo Wang, Xiaoyu Cheng, Yun Ding,* and Aiguo Hu*

Cite This: J. Org. Chem. 2021, 86, 1549−1559 Read Online

ACCESS | Metrics & More | Article Recommendations | Supporting Information

ABSTRACT: The follow-up reaction pathways of the diradical species formed from cycloaromatization of enediynes or enyne−allenes determine their ability of H-abstraction from DNA, significantly affecting their biological activity performance. To gain a deeper understanding of subsequent reaction pathways of the diradical intermediates formed from acyclic enediynes based on maleimide-assisted rearrangement and cycloaromatization (MARACA), a maleimide-based enediyne featuring methylene groups adjacent to the propargyl sites of the terminal alkynes was synthesized through the Sonogashira coupling reaction. Three thermal cyclization products after intramolecular hydrogen atom transfer (HAT) were obtained from the thermolysis experiment and their structures were confirmed by 1D and 2D nuclear magnetic resonance spectroscopic analysis. Density functional theory was employed to analyze the important elementary steps including rearrangement, cycloaromatization, and intramolecular HAT processes toward the formation of the cyclized products, where the low-energy barriers of HAT pathways relative to the formation of diradicals from cycloaromatization were successfully identified. Overall, the HAT processes to consume diradicals intramolecularly have become competitive with that of intermolecular H-abstraction, implying that the DNA-cleavage ability of enediynes can be further boosted once the HAT processes are halted. This study offers a promising direction for designing novel and potent acyclic enediynes for antitumor applications.

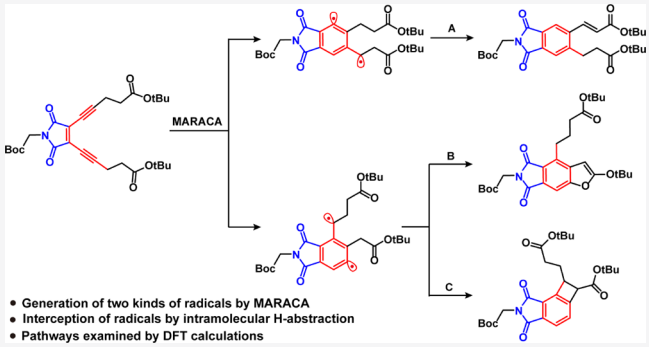

INTRODUCTION

Since their discovery in the 1980s from natural resources, enediynes have drawn intensive attention because of their high potential as a class of cytotoxic antitumor agents.[1,2] The special feature of cycloaromatization of the enediyne structural scaffold, generating reactive radical species from closed-shell molecules,[3] endows it with extraordinary cytotoxicity against a broad range of tumor cells. The 1,4-benzene diradicals generated from the 1,6-cyclization of enediynes, known as Bergman cyclization (BC),[4−6] are able to abstract H or halogen atoms from suitable small molecules, for example, 1,4-cyclohexadiene (CHD) and haloalkanes,[7] which is the fundamental mechanism of their biological activity when the carbohydrate moieties in the DNA backbone behave as the H-donors. As a result, the naturally occurring enediynes with profound DNA-damaging activities are hailed as the most active molecules among all the known cytotoxic agents. Indeed, one of the natural enediynes, calicheamicin, has been used as the "warhead" of chemotherapeutic agents (Mylotarg and Besponsa) for the clinical treatment of leukemia after conjugation with the monoclonal antibody.[8,9] Unfortunately, the development of enediyne-based chemotherapy remains hampered by the scarcity of isolation from natural resources and the difficulty of their construction for a complicated 9 or 10-membered cyclic architecture through total synthesis.[10−12]

Many endeavors that explore analogues of natural enediynes with simple structures and high efficiency have been made so far and are still ongoing.[1,13−16] Among them, a variety of activation strategies such as cycle constriction,[17] strain release,[18] and protecting/deprotecting of a triple bond[19] were considered in the design of enediyne structures in order to balance the stability and reactivity. On the other hand, Myers−Saito cyclization (MSC)[20,21] of enyne−allene plays a key role in the bioactivity of natural enediynes like neocarzinostatin (NCS).[22] Moreover, the highly reactive enyne−allene can be transformed from the enediyne unit via

Received: October 10, 2020
Published: December 29, 2020

Downloaded via UNIV OF NEW MEXICO on May 15, 2021 at 00:04:07 (UTC).
See https://pubs.acs.org/sharingguidelines for options on how to legitimately share published articles.

© 2020 American Chemical Society

https://dx.doi.org/10.1021/acs.joc.0c02401
J. Org. Chem. 2021, 86, 1549−1559

Scheme 1. Structure of EDY-B and the Synthesis of Enediyne Compound EDY-A: (a) $LiNPr_2^i$, HMPA, $CH{\equiv}CCH_2Br$, Tetrahydrofuran (THF), −78 °C, 3 h; (b) $BocCH_2NH_2{\cdot}HCl$, Potassium Acetate, Acetic Acid, 40 °C, 40 h; (c) NaI, Acetonitrile, Reflux, 12 h; and (d) $(PPh_3)_2PdCl_2$, CuI, *N,N*-Diisopropylethylamine (DIPEA), Toluene/THF, r.t., 6 h

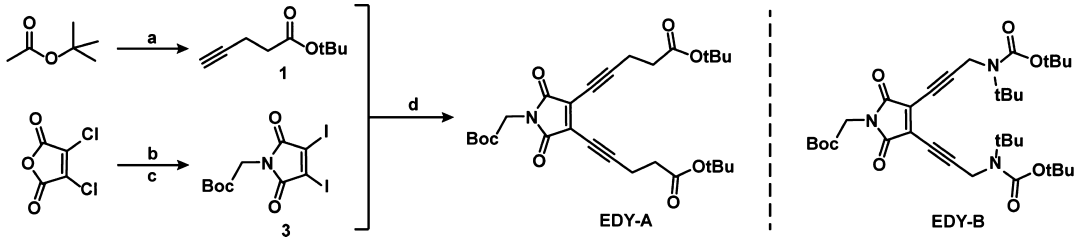

propargyl−allene rearrangement, and immediately undergoes MSC to afford α,3-didehydrotoluene diradicals at relatively lower temperature. Notably, the isomerization process of enediynes to enyne−allenes occurring under mild conditions is of special importance for their biological and medical applications. However, this transformation typically requires an acid, a base, an oxidant, transition metal complexes, or heating at high temperature,[23−26] many other organocatalytic approaches are also possible for this tautomerization,[27,28] and these activation conditions are not accessible to the biological environments. Recently, a new strategy, maleimide-assisted rearrangement and cycloaromatization (MARACA) triggering the antitumor activity of acyclic enediynes, has been uncovered in our work.[29] This approach allows the propargyl−allene isomerization to be greatly promoted by installing a maleimide group at the ene position of enediynes, making the otherwise inactive acyclic enediynes undergoing MSC under physiological conditions.

Once the diradical species are produced from facile MSC of enyne−allenes, another important aspect concerning the consumption pathways of these reactive species should be paid attention to, because the fate of the diradicals is closely related to their DNA cleavage activity and the ultimate cytotoxic performance. Diradicals that have no self-quenching mechanism would undergo H-abstraction from external sources (such as DNA backbones). On the contrary, the chances of diradicals to interact with external sources would be severely reduced if any kind of intramolecular radical transfer pathways exist. Indeed, a variety of intramolecular radical self-quenching cases have been found in different enyne−allene systems.[30−32] Among them, the intramolecular hydrogen atom transfer (HAT) reactions were generally involved as the elementary step, which lead to the consumption of diradicals.[33] On the other hand, the intramolecular capture of transient phenyl radicals via HAT reactions has been proved as an activation mechanism of natural enediyne antibiotics prodrug depending on a favorable conformational change.[34] The resulting irreversible cycloaromatization renders the newly formed radical center a longer lifetime for abstracting H from external sources.

In our early efforts of screening maleimide-based acyclic enediynes with antitumor potencies, the focus was mainly on the steric and electronic effects of the functionalities close to the alkyne termini to tune the cycloaromatization reactivity.[35−38] As for the new MARACA mechanism guiding the design of various enediynes with potent anticancer activity, it is essential to gain insight into the fate of the diradical species after their cycloaromatization. Herein, the follow-up intramolecular radical transfer processes of enediynes after MARACA have been investigated. Three possible pathways directing the diradicals to stable products involving intramolecular HAT steps are elaborated experimentally and computationally. A deeper understanding of these intramolecular reaction pathways would provide a guideline for exploring and designing novel enediyne compounds with H-abstraction ability close or even comparable to natural enediynes like calicheamicin and high potential for antitumor applications.

RESULTS AND DISCUSSION

Synthesis of Enediynes. Encouraged by the MARACA strategy demonstrated in our previous work,[29] the same maleimide functionality was installed at the ene position to assist the transformation of the inert enediyne core into the highly reactive enyne−allene structure. Because the substituent effect at the propargyl site plays a vital role in the reactivity of the rearrangement and cycloaromatization processes,[3,39] two terminal alkynes, *tert*-butyl pent-4-ynoate (**1**) and prop-2-yn-1-yl acetate (**2**), featuring carbon and oxygen atoms at the propargyl site, respectively, were used in the construction of enediyne compounds, which is distinct from **EDY-B**[29] that has a nitrogen atom at the same position (Scheme 1). Compounds **1**[40] and **3**[41] were synthesized using the literature-reported procedures without any modification. The Sonogashira coupling reaction between alkyne **1** and alkene **3** occurred to give **EDY-A** with a moderate yield at ambient temperature (Scheme 1). Meanwhile, compound **4** with bright blue fluorescence was detected by thin layer chromatography (TLC) (vide infra) even at the early stage of this reaction. Similar to the in situ enyne−allene tautomerization strategy described in our previous work,[29] the transformation of **EDY-A** into compound **4** and a trace amount of mixed compounds **5** and **6** was also observed with increased reaction time. Interestingly, when the transformation process was carried out at an elevated temperature, the mixtures of compounds **5** and **6** were isolated as the major products. In contrast to the transformation of **EDY-B** into the corresponding cyclized product, a longer reaction time or a higher reaction temperature was needed in the **EDY-A** system. The molecular structure of **EDY-A** was confirmed with nuclear magnetic resonance spectroscopy (NMR) and high-resolution mass spectra (HRMS) analysis (Supporting Information). The structures of compounds **4**, **5**, and **6** were characterized by 1D, 2D NMR, and HRMS analyses. More detailed analysis of these cyclized products would be discussed below. On the other hand, when similar experimental procedures were subjected to the Sonogashira coupling between alkyne **2** and diiodomaleimide **2S**, the only separable small molecular product was the monosubstituted maleimide by the terminal alkyne **2** (Scheme S1). As demonstrated earlier by our group

https://dx.doi.org/10.1021/acs.joc.0c02401
J. Org. Chem. 2021, 86, 1549−1559

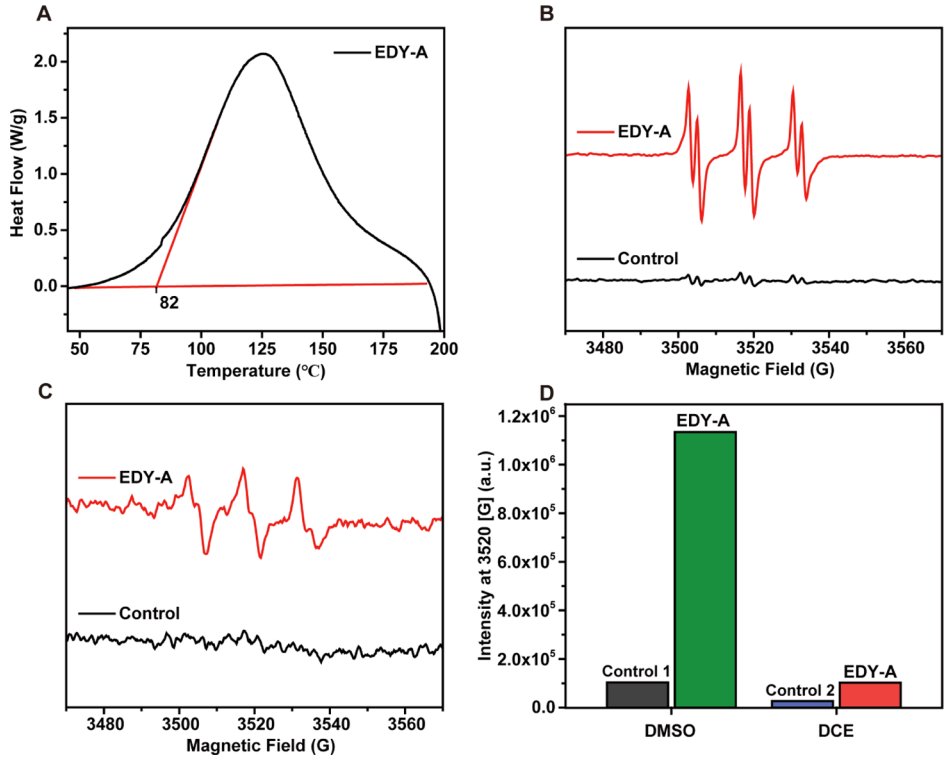

Figure 1. (A) DSC curve of **EDY-A** determined at a heating rate of 10 °C/min. The baseline is marked in red. (B) EPR spectra of control and **EDY-A** (20 mM) in the presence of PBN (100 mM) in DMSO at 37 °C for 12 h. (C) EPR spectra of the samples in DCE under the same experimental conditions. (D) EPR signal intensities at 3520 G of samples in DMSO and DCE, respectively.

and others, the enediynes with propargyl groups could be smoothly synthesized under the Sonogashira conditions when the benzene or vinyl group functions as the alkene source,[42−46] meanwhile, asymmetric maleimide-based enediynes with propargyl ester at one of the two arms were synthesized in a good yield.[38] Therefore, the failure of synthesizing maleimide-based enediynes with symmetrical propargyl substituents implies the significant effect of the maleimide moiety on the relationship between the structure and reactivity of the enediynes. A minor modification of the substituents at the yne termini of maleimide-based enediynes would lead to a dramatic change in the reactivity of rearrangement and cycloaromatization. Nonetheless, deeper experimental and computational studies are needed to clarify these issues.

Thermal Reactivity of Enediynes. The thermal reactivity of enediynes was evaluated using differential scanning calorimetry (DSC). It could provide the onset temperatures of the enediynes or enyne−allenes corresponding to radical polymerization after their thermal cycloaromatization processes,[47,48] which is the alternative method for qualitative evaluation of the reactivity in solution. For example, **EDY-A** and its analogue **EDY-C** (replacement of the Boc group in **EDY-A** with a phenyl substituent, Scheme S2) equipped with the same alkyne functionalities share a similar onset temperature at ∼80 °C (Figures 1A and S1), indicating that the onset temperatures determined by DSC are not affected by the *N*-substituents of maleimide. In contrast, **EDY-B**, bearing the identical structure of **EDY-A** except for the N atom at the propargyl site, showed a relatively low onset temperature at 56 °C.[29] The higher reactivity of **EDY-B** may be attributed to the hyperconjugative effects of σ-acceptors (donation from alkyne to the σ^*_{C-N} orbitals).[49] As described in the MARACA mechanism, the propargyl−allene tautomerization is greatly assisted when the maleimide moiety functions as the ene source in the acyclic enediynes, ultimately shifting the reaction pathway from BC to MSC. Thus, the cyclization mode of both enediynes is attributed to the MSC behavior, dramatically lowering the cycloaromatization reaction temperatures in comparison to that of BC mode. Moreover, it is worth noting that the electronic effect of the substituents at the propargyl position influences the MSC reactivity significantly, according to DSC experiments performed at different onset temperatures. This observation of the relative reactivity of two enediynes using DSC is in good agreement with the activation barriers obtained using density functional theory (DFT)[50,51] calculations, where the value of activation energy for **EDY-B** in the MSC is 1.6 kcal/mol lower than that of **EDY-A** (see in Table 1).

Table 1. Activation Energy Values (kcal/mol) for the MSC of Enediynes

		ΔG	
entry	X	MSC1	MSC2
1	C	26.3	27.6
2	N	24.0	26.0
3	O	24.4	20.5

Detection of Radical Intermediates. As mentioned above, **EDY-A** undergoes thermal cycloaromatization at a relatively low temperature. Next, the electron paramagnetic resonance (EPR) spectroscopy[52] was used to examine the possibility of producing radicals from enediynes.

Generally, it is hard to directly detect these radical species in situ because of the short lifetime and high reactivity[53,54] in this

https://dx.doi.org/10.1021/acs.joc.0c02401
J. Org. Chem. 2021, 86, 1549−1559

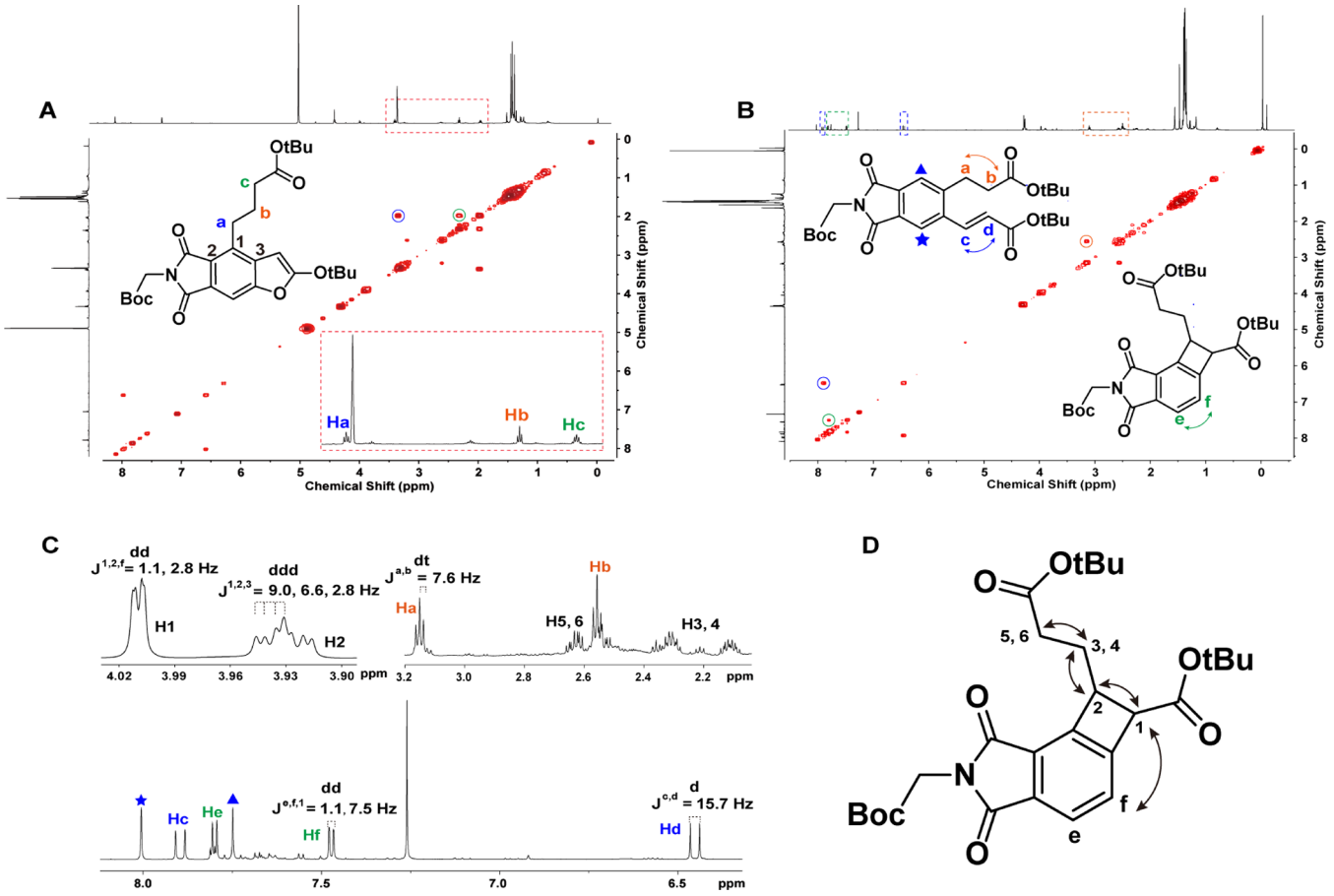

Figure 2. (A) ^{1}H−^{1}H COSY spectrum of compound **4**. Inset is the enlarged ^{1}H NMR spectrum. (B) ^{1}H−^{1}H COSY spectrum of compounds **5** and **6**. (C) ^{1}H NMR analysis of compounds **5** and **6**. (D) Key ^{1}H−^{1}H correlations for compound 6.

special type of reactions. Thus, *N-tert*-butyl-alpha-phenyl-nitrone (PBN) was exploited as a spin trap agent to convert the transient species into stable radical adducts.[55,56] For the preparation of samples for EPR studies, **EDY-A** (1 equiv) was dissolved in dimethyl sulfoxide (DMSO) and 1,2-dichloro-ethane (DCE) with the addition of excess PBN (5 equiv) to each sample. After that, the samples were placed at 37 °C for 12 h before EPR measurement. As can be seen in Figure 1B, strong and typical triplet-doublet signals with a hyperfine splitting constants of 14.2 and 2.3 G were observed, suggesting the formation of nitroxide radicals relative to spin-trapped PBN adducts with diradicals generated from the cyclo-aromatization of enediynes. This value is similar to that reported for the calicheamicin phenyl radical adduct with PBN (A_N = 14.2 G, A_H = 2.6 G).[56] On the contrary, when the mixture of **EDY-A** and PBN was warmed at 37 °C in a nonpolar solvent DCE, the EPR signals appear much weaker (Figure 1C). Figure 1D displays the recorded intensity at 3520 G for **EDY-A** in two different solvents, indicating that the generation of free radicals is strongly dependent on the solvent polarity. This observation is because of the existence of polar intermediates in the propargyl−allene tautomerization processes, and the polar solvent is beneficial to the rearrangement behavior.

Scheme of Intramolecular HAT after MARACA and Cyclized Products. The cyclized products **4**, **5**, and **6** were initially obtained in a one-pot manner through a tandem Sonogashira coupling reaction, followed by propargyl−allenyl tautomerization, cycloaromatization, and eventually intra-molecular HAT processes. When **EDY-A** was dissolved in CHD to a final concentration of 10 mM and the reaction system was heated at 80 °C for 3 d, a mixture of these three cyclized products was equally formed as those from the tandem reactions. No relevant radical H-abstraction product was isolated even if **EDY-A** was exposed to a large excess of CHD, which suggests that when an intramolecular radical cyclization/H-abstraction path is involved in the fate of the diradical intermediate, the intermolecular H-abstraction may became less efficient regardless of the cycloaromatization modes.[47,57,58] On the other hand, because of the similarities of the cyclized products in molecular structure and polarity, it is very difficult if not impossible to separate out each compound in pure form by column chromatography. To characterize the accurate structures from the isolated mixed compounds, 2D NMR correlation experiments, including heteronuclear single quantum coherence (HSQC), heteronuclear multiple bond correlation (HMBC), and ^{1}H−^{1}H correlation spectroscopy (COSY), have been carried out (Figure 2 and Supporting Information).

Take the ^{1}H−^{1}H COSY analysis for example, it provides clear and crucial proton correlations, allowing the assignment of vital structural fragment when combining with the *J*-coupling data from ^{1}H NMR. In the ^{1}H−^{1}H COSY spectrum (Figure 2A), the correlation information of H_a/H_b and H_c/H_b, together with HMBC correlations of H_a/C_b, C_c, C_1, C_2, and C_3 (Supporting Information), confirmed the connection of the

https://dx.doi.org/10.1021/acs.joc.0c02401
J. Org. Chem. 2021, 86, 1549−1559

Scheme 2. Outline of Intramolecular HAT Pathways to Form the Cyclized Products 4, 5, and 6

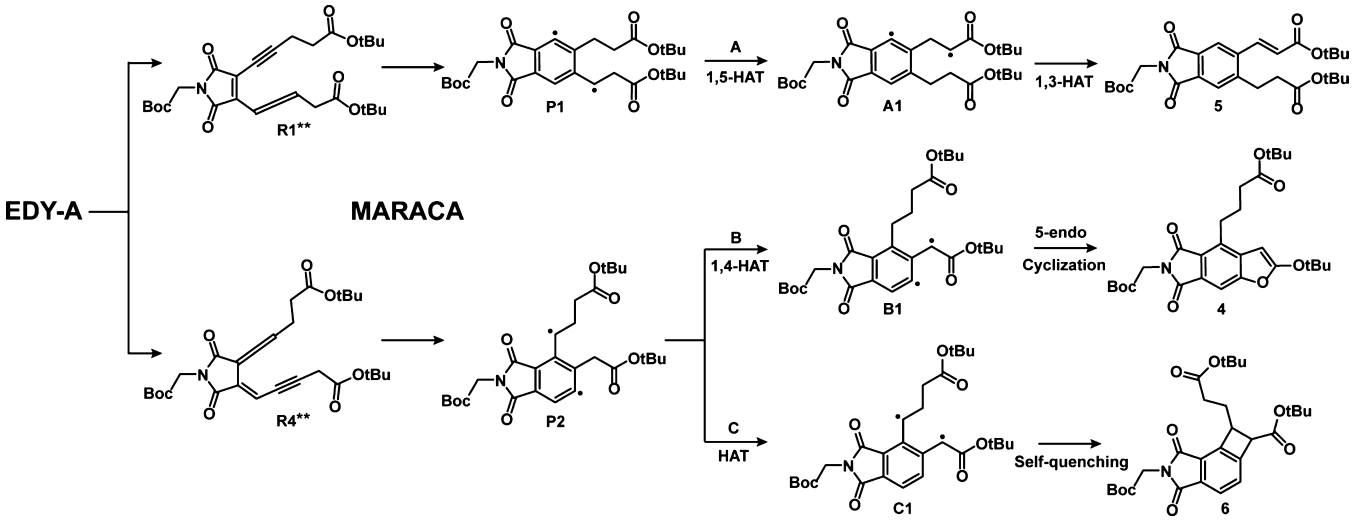

ester moiety to a newly formed aromatic ring subunit as depicted in structure **4**. Similarly, Figure 2B,C illustrates the proton correlations, which help us to distinguish structures between two mixed compounds **5** and **6**. For instance, the distinct H_a/H_b and H_c/H_d cross peaks of compound **5** could be observed in the $^1H-^1H$ COSY spectrum (Figure 2B). The coupling constant between H_a and H_b (7.6 Hz) indicates that the two protons are adjacent in position (Figure 2C). Besides, the large vicinal coupling constant (15.7 Hz) between H_c and H_d reveals that the double bond is in trans configuration as depicted in compound **5**, identifying from the coupling constant range of 3−13 Hz for cis and 12−20 Hz for trans alkenes.[59] In this case, once the configuration of compound **5** was determined by interpretation of its COSY spectrum, the other structure is prone to be recognized by using the remaining information of the 1D and 2D NMR data. First, an obvious H_e/H_f cross peak with a vicinal coupling constant (7.5 Hz) strongly indicates that these protons belong to a tetra substituted phenyl ring (Figure 2B,C). Apart from H_e and H_f, another two tertiary hydrogen H_1 and H_2 were assigned to construct the cyclobutane part, on the basis of DEPT, HSQC, and HMBC analyses (Figure 2D and Supporting Information). Figure 1C gives the detailed coupling information between correlative protons, in which the small coupling constant (1.1 Hz) between H_1 and H_f means the presence of long-range coupling. Moreover, the rotation along single bonds is probably restricted in the cyclobutane subunit, resulting in the complexity of ^1H NMR signals in H_3, H_4, H_5, and H_6, evidenced in the displayed spectrum of a similar benzofused cyclobutane moiety.[60] H_2 has correlations with H_1, H_3, and H_4, corresponding to coupling constants of 2.8, 6.6, and 9.0 Hz, respectively, matching well the assigned structure **6**. The sample of mixed compounds **5** and **6** was further evaluated by the high-performance liquid chromatography−mass spectrometry (HPLC−MS) method, accessible to two main peaks belonging to compounds **5** and **6** (Figure S2).

According to the MARACA mechanism for maleimide-based enediynes, two kinds of α,3-didehydrotoluenes derivatives **P1** and **P2** could be generated from **EDY-A**, and these diradicals would further undergo either an intramolecular or an intermolecular consumption pathway. After the formation of diradical species, the possible pathways A−C shown in Scheme 2 would explain the mixture of obtained compounds **4**−**6** accordingly. Pathway A proceeds through an intramolecular 1,5-HAT from **P1** to give another diradical intermediate **A1**, which intermediately undergoes 1,3-HAT to afford the closed-shell product **5**. Apart from forming compound **5**, there is a possibility of the formation of a cyclobutane ring counterpart by the radical coupling from intermediate **A1**. To this end, the simulated NMR spectrum of the possible cyclobutane ring structure (Figure S3) indicated that the H_1 signal should locate between 7.5−8.0 ppm as a sharp singlet peak. Meanwhile, there are some unidentified signals after assignment of these major peaks to compounds **5** and **6**, probably accounting for other unseparated/unidentified compounds under these experimental conditions because of the complexity of free radical-involved reaction pathways. Altogether, the formation of a cyclobutane ring product from **A1** cannot be ruled out, but the amount of this compound could be very small. For the cases starting from **P2**, pathway B involves the 1,4-HAT to yield intermediate **B1** followed by 5-endo radical cyclization to form compound **4**. A second path from **P2** is the pathway C that leads to the formation of compound **6** via HAT assisted by the carbonyl group and subsequent self-quenching process of diradical intermediate **C1**. As a consequence, the three pathways dominate the consumption of reactive free radical species intramolecularly by means of various HAT routes.

Computational Study. DFT calculations were carried out to examine the possible pathways to understand the proton transfer processes and the reactivity of the cycloaromatization reaction as well as the intramolecular hydrogen shift reactions to explain the formation of the cyclized products. The structurally simplified models have been used to carry out the computational studies (Scheme S3 and Figure S4), in which the acetate anion serves as the proton shuttle to assist the rearrangement processes. DFT calculations have been performed in the Gaussian 09 package[61] at the (U)B3LYP/6-31G(d) level. Specifically, a restricted method was used for geometry optimization of the closed-shell molecules, while for a variety of other geometries possessing the open-shell character, including the transition states (TS) of the MSC and HAT processes and all biradical intermediates, an unrestricted broken-symmetry approach with the "guess = (mix, always)" designation has been utilized. The optimized geometries are all verified to be either minima (no imaginary frequencies) or TSs (one imaginary frequency) via frequency

https://dx.doi.org/10.1021/acs.joc.0c02401
J. Org. Chem. 2021, 86, 1549−1559

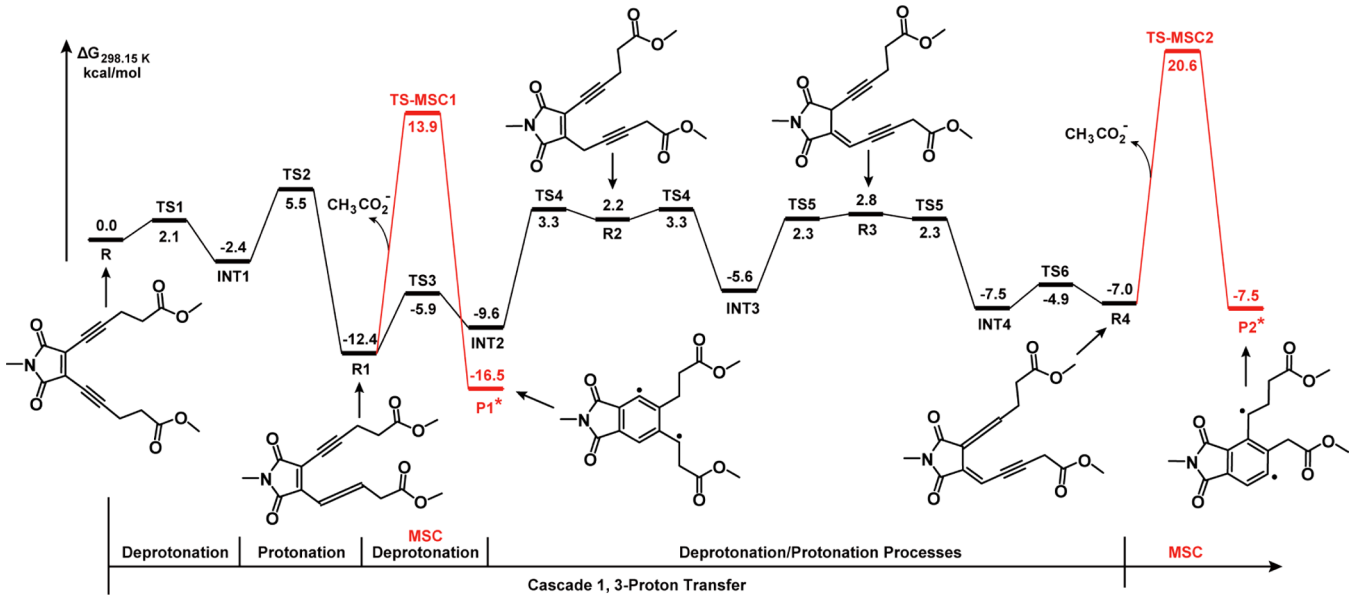

Figure 3. Gibbs free energy profile (kcal/mol) for rearrangement (black lines) and MSC (red lines) processes in Scheme S3. All the optimized structures for stationary points can be found from Figure S4.

Scheme 3. Two MSC Pathways From Their Corresponding Enyne−Allene Precursors and the Initial Enediyne Model R

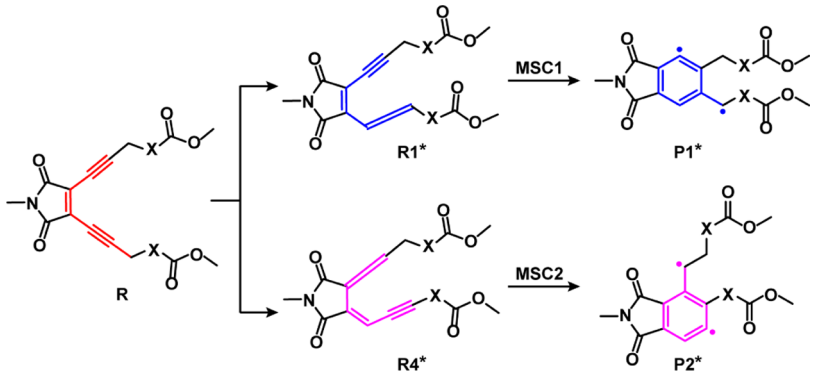

calculations at 298.15 K. Moreover, intrinsic reaction coordinate (IRC) calculations were carried out to confirm the connection of these TSs to two directions of reactants and products. The solvent effects of toluene and THF were also considered by employing a polarizable continuum model (PCM)[62] with the self-consistent reaction field (SCRF) method[63] based on the optimized structures in the gas phase at the (U)B3LYP/6-31G(d) level. However, the solution-phase single-point energy calculations were accomplished at a higher level ((U)M06/6-311++G(d,p)). This method suited for application in the mechanistic studies of proton transfer reaction[64] and the resulting Gibbs free energy in solvents (toluene and THF) was computed with reference to the known method in the literature.

As shown in Figure 3, prior to the formation of diradical intermediates via a cycloaromatization reaction (red line), the substrate **R** (similar to **EDY-A**) would proceed isomerization to enyne−allene **R1** and **R4**, respectively, via a 1,3-proton shift with the help of acetate anion (black lines). Take the first tautomerization of the propargyl group in enediyne **R** to form the enyne-allene **R1** as an example. With the assistance of the proton shuttle, the abstraction of propargyl protons from **R** occurs over **TS1** (2.1 kcal/mol), causing the formation of **INT1**. Immediately, the isomerization to enyne−allene **R1** is completed by protonation with a small barrier of 7.9 kcal/mol. Once the precursor **R1** for MSC is formed, the cycloaromatization would take place to give diradical **P1*** through **TS-MSC1**. Similarly, the other path to afford **P2*** needs to undergo further 1,3-proton transfer steps and cycloaromatization reaction. In the whole MARACA reaction, the MSC step has the highest energy barrier of 27.6 kcal/mol, and the proton transfer processes are accessible because of the low activation barriers. Meanwhile, it is noteworthy that the involved polar intermediates in the rearrangement processes should be responsible for the observed solvent dependence in the EPR performance.

DFT Calculations for the Evaluation of MSC Reactivity for Enediynes. Judging from the above computational results, the highest energy barrier in the MARACA mechanism lies in the MSC step. To estimate the relative stability/reactivity balance of enediynes, the DFT computed activation energies for MSCs (directly formed from structure **R1** as MSC1 and from structure **R4** as MSC2, Scheme 3) are given in Table 1. Calculations revealed that different atoms at the propargyl site affect the MSC reactivity significantly especially for the latter case. When the heteroatoms (N, O) are placed at the propargyl position of enediynes, the energy barrier values are close and only ∼2 kcal/mol lower than that of the C atom

https://dx.doi.org/10.1021/acs.joc.0c02401
J. Org. Chem. 2021, 86, 1549−1559

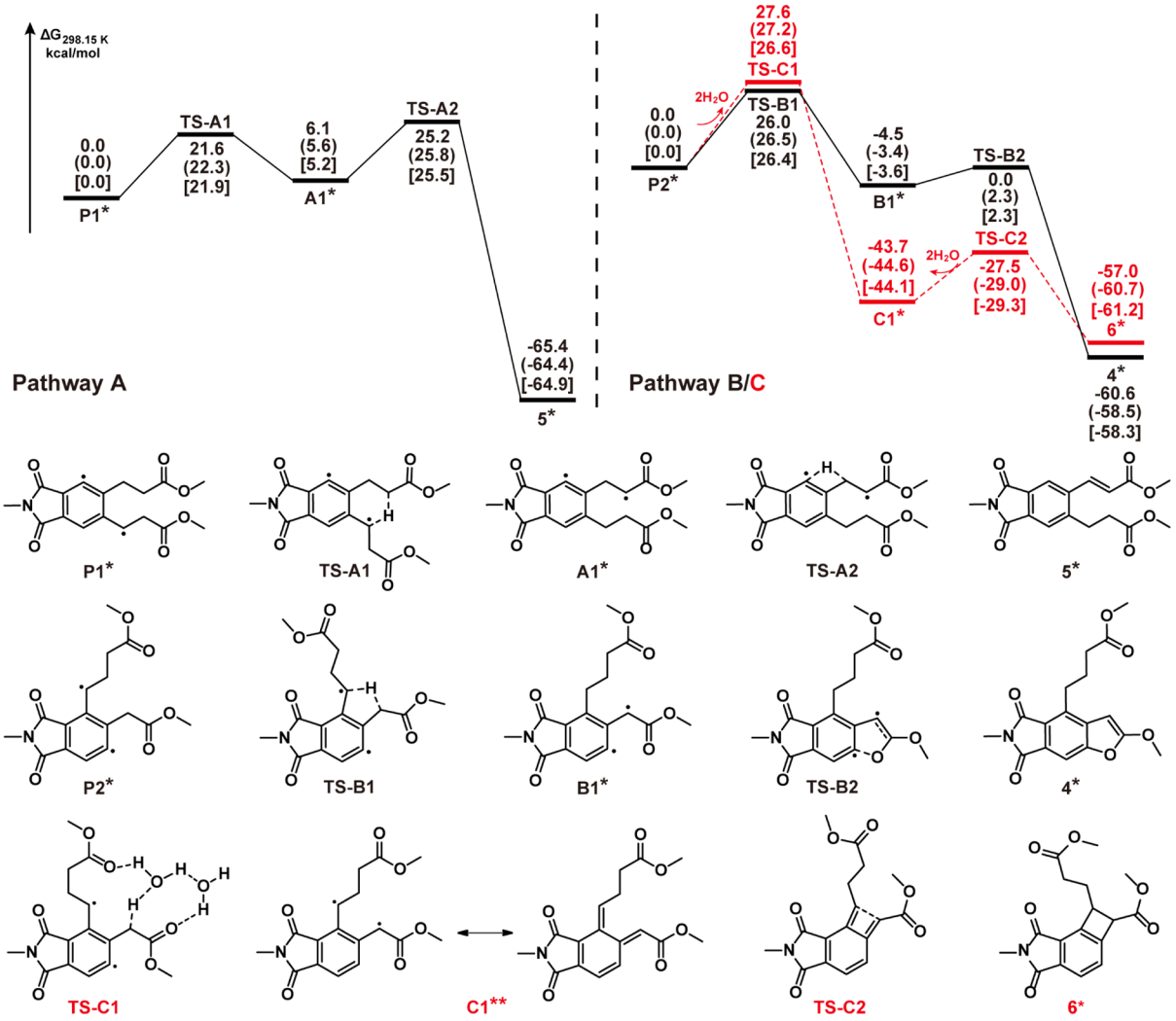

Figure 4. Gibbs free energy profile (kcal/mol) of HAT pathways A, B, and C to form products **5***, **4***, and **6*** starting from **P1*** and **P2***, respectively. The values of Gibbs free energy calculated in the gas phase are shown in the normal text, while the ones calculated in toluene are in parentheses, and the ones calculated in THF are in brackets.

in the MSC1 situation. However, the activation energy values calculated for MSC2 show relatively large differences. While the structure bearing the methylene group at the propargyl site has the highest activation barrier value of 27.6 kcal/mol (Table 1, entry 1), the other two structures have the values of 26.0 and 20.5 kcal/mol, respectively (Table 1, entries 2 and 3). Reference to the results from Table 1, we can conclude that the MSC reactivity order of enediynes is C < N < O according to the activation energy values. Meanwhile, these results are consistent with what has been observed in the DSC experiments that the onset temperature of **EDY-A** is 26 °C higher than that of **EDY-B**. These findings could prove the relative stability/reactivity scale of maleimide-based enediynes, providing an "optimal structure" with a good reactivity along with a reasonable stability for exploring compounds for biological applications.

Upon the formation of diradicals **P1*** and **P2*** through the MARACA strategy, the follow-up reaction pathways of the two kinds of diradicals toward **5*** and **4*** were examined by computational studies, respectively (Figure 4). First of all, the intramolecular 1,5-HAT relative to the benzyl radical may occur over **TS-A1** (21.6 kcal/mol) through an open-shell singlet diradical pathway yielding intermediate **A1***, followed by 1,4-HAT with a barrier of 19.1 kcal/mol to give the closed-shell product **5*** (Pathway A). Indeed, the 1,3-HAT process is unfavorable and relevant examples are rather scarce because the process occurs accompanying the highly strained and distorted four-membered-ring transition structure.[65,66] The 1,3-HAT barrier of a similar structure **A1**** (the absence of the carbon radical adjacent to the carbonyl group) has also been calculated for comparison (Figure S5). Unsurprisingly, the activation energy of 1,3-HAT (36.8 kcal/mol) for **A1**** is high. Thus, the presence of one radical adjacent to the carbonyl group in **A1*** seems to accelerate the 1,3-HAT process, making it possible to be a thermal process in this special case. Likewise, pathway B also discloses the two-step radical transfer mechanism involving the 1,4-HAT and 5-endo cyclization processes, eventually leading to the formation of **4***. Besides, along the reaction paths, the transition states **TS-A1**, **TS-A2**, **TS-B1**, and **TS-B2** all exhibit the open-shell characteristics, and the typical diradical characteristics in the intermediates **A1*** and **B1*** were observed from the spin density distributions (Figure 5), confirming the free radical-involved pathways.

For diradical **P2***, a competitive consumption pathway to give **6*** is proposed apart from the path to **4***. After careful

https://dx.doi.org/10.1021/acs.joc.0c02401
J. Org. Chem. 2021, 86, 1549−1559

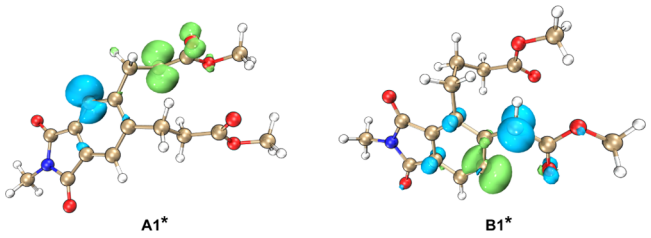

Figure 5. Spin density plots for intermediates **A1*** and **B1***.

consideration of the structure of compound **6**, a unimolecular 1,3-H shift is taken into account by DFT calculations (Figure S6), leading to the radical relocation from the phenyl to benzyl position. However, the one-step radical transfer should be ruled out because of the high activation energy of 35.4 kcal/mol. Alternatively, the possibility of the radical transfer assisted by the carbonyl group was examined. As expected, the activation energy of direct keto-enol tautomerization induced by proton transfer is calculated to be as high as 68.5 kcal/mol, comparable to reported cases.[67] Given the ability of water molecules serving as the proton donor and acceptor simultaneously,[68] single or two water molecules are considered as the effective proton shuttle in such a reaction system to catalyze the keto-enol transformation, respectively. Calculations indicate that one water decreases the activation energy to 40.4 kcal/mol, and the latter case of involving two water for the interconversion shows a far lower barrier of 27.6 kcal/mol, attributing to the acetoxy group around the reaction active site functioning as a proton acceptor to stabilize the hydrogen bond network, which is the lowest energy pathway identified toward intermediate **C1****. It is noticeable that the enol formed from keto-enol tautomerization of the above three cases cannot be obtained from structural optimization. DFT calculations only afford the further H-abstraction structure **C1*** with the absence of any unpaired electron. In fact, the intermediate **C1*** and its diradical resonance structure similar to the Garratt−Braverman cyclization[69] intermediate would undergo intramolecular reaction to form **6*** via either diradical self-quenching or formal [2+2] cycloadditions[70] with a barrier of 16.2 kcal/mol over **TS-C2**. Overall, the DFT calculation results suggest that the diradicals formed from MSC could become diamagnetic through various HAT pathways depending on the substrates, eventually yielding the thermodynamically stable products.

CONCLUSIONS

In summary, the maleimide-based acyclic enediynes are able to generate diradical species through the MARACA strategy under mild conditions. The effect of solvent polarity on the cascade rearrangement and cycloaromatization was revealed, and the polar solvent was found to accelerate the generation of free radicals from the EPR studies. Subsequent thermolysis experiment of enediynes provided three kinds of intramolecular HAT products. The formation pathways of these products from open-shell diradical intermediates have been verified using theoretical calculations. During the radical transformation, the highest energy barrier for intramolecular H-abstraction steps is 27.6 kcal/mol, posing a powerful competition with external H-abstraction behavior from either thermodynamic or kinetic aspect. This probably is the reason for the relatively low cytotoxicity of currently developed maleimide-based enediynes in comparison with natural enediynes (IC_{50} values of submicromolar vs nanomolar level). By combining the experimental and computational results, this investigation on intramolecular radical transfer pathways of maleimide-based acyclic enediynes would provide a guidance for the discovery of novel structurally simple yet more powerful enediyne antitumor agents, which is underway in our group.

EXPERIMENTAL SECTION

General Methods. Toluene and THF were dried over calcium hydride (CaH_2) and distilled before use. Other reagents were purchased from commercial sources. Sonogashira reactions were conducted under a nitrogen atmosphere. ^1H and $^{13}C\{^1H\}$ NMR spectra of all compounds were reported in ppm at 400 or 600 MHz (Bruker) using deuterated solvents ($CDCl_3$: δ_H = 7.26, δ_C = 77.2 ppm; CD_3OD: δ_H = 3.31, δ_C = 49.0 ppm) as reference. Structural assignments for compounds **4**, **5**, and **6** were made with additional information from gHSQC and gHMBC experiments. HRMS data were recorded on the Micromass LCTTM mass spectrometer using the ESI method. EPR studies were performed with an X-band EMX-8/2.7C spectrometer (Bruker). DSC experiments were investigated with the Pyris Diamond thermal analysis workstation. DSC samples were studied with the heating rate of 10 °C/min ranging from −10 to 250 °C under a flow of nitrogen. The new compounds (**EDY-A**, **3S**, and **EDY-C**) were synthesized following our previous general procedures for the Sonogashira coupling reaction with minor modifications.[29]

***Tert*-butyl Pent-4-ynoate (1).**[40] *N*-Butyllithium (2.7 M in hexane, 9.6 mL, 26 mmol) was added to Pri_2NH (4.2 mL, 30 mmol) in THF (120 mL) under N_2 at −78 °C. After 30 min, *t*-butyl acetate (2.6 g, 22 mmol) was added and the mixture was stirred for 1 h at −78 °C. After that, HMPA (10.4 mL, 60 mmol) was added and stirred for 10 min followed by the addition of 3-bromo-1-propyne (2.4 g, 20 mmol) dropwise. The reaction system was held at −78 °C for another 1 h, then warmed to room temperature. In the end, the reaction was quenched with the saturated NH_4Cl solution (5.0 mL) before the mixture was diluted with hexane (100 mL), and then washed with HCl (1.0 M, 2 × 50 mL) and brine (2 × 50 mL). The resulting organic phase was dried over $MgSO_4$, filtered, and the solvent was evaporated under reduced pressure to give **1** as a yellow oil (2.4 g, 79%). ^1H NMR (400 MHz, $CDCl_3$): δ 2.43 (m, 4H), 1.94 (m, 1H), 1.43 (s, 9H); $^{13}C\{^1H\}$ NMR (151 MHz, $CDCl_3$): δ 171.2, 82.9, 81.0, 68.9, 34.6, 28.2, 14.6.

Di-*tert*-butyl 5,5′-(1-(2-(*Tert*-butoxy)-2-oxoethyl)-2,5-dioxo-2,5-dihydro-1*H*-pyrrole-3,4-diyl)bis(pent-4-ynoate) (EDY-A). The **EDY-A** was synthesized by Sonogashira coupling between compounds **3** and **1**. The mixture was stirred at ambient temperature until completion of the reaction as detected by TLC (6 h). After that, the mixture was subjected to silica gel chromatography (hexane/ethyl acetate = 6:1) to give a yellow oil (150 mg, 58%). ^1H NMR (400 MHz, $CDCl_3$): δ 4.12 (s, 2H), 2.79 (t, J = 7.5 Hz, 4H), 2.54 (t, J = 7.5 Hz, 4H), 1.43 (s, 18H), 1.40 (s, 9H); $^{13}C\{^1H\}$ NMR (151 MHz, $CDCl_3$): δ 170.6, 166.7, 165.9, 128.6, 110.2, 83.0, 81.2, 71.8, 40.2, 33.9, 28.1, 28.0, 16.5; HRMS (ESI-TOF) m/z: $[M + Na]^+$ calcd for $C_{28}H_{37}NO_8Na$, 538.2417; found 538.2416.

***Tert*-butyl 4-(2-(Tert-butoxy)-6-(2-(tert-butoxy)-2-oxoethyl)-5,7-dioxo-6,7-dihydro-5*H*-furo[2,3-f]isoindol-4-yl)-butanoate (4).** Isolated by silica gel chromatography (hexane/ethyl acetate = 6:1) to give a yellow solid (24 mg, 9%) from the synthesis procedure of **EDY-A** in which the reaction system was further heated to 37 °C in an oil bath for a week. ^1H NMR (600 MHz, CD_3OD): δ 7.82 (s, 1H), 7.07 (s, 1H), 4.32 (s, 2H), 3.35 (t, J = 7.7 Hz, 2H), 2.32 (t, J = 7.2 Hz, 2H), 1.98 (m, 2H), 1.49 (s, 9H), 1.47 (s, 9H), 1.43 (s, 9H); $^{13}C\{^1H\}$ NMR (151 MHz, CD_3OD): δ 174.4, 169.4, 168.9, 168.5, 158.2, 157.8, 137.5, 135.9, 130.1, 124.3, 106.5, 106.0, 83.7, 83.2, 81.6, 40.5, 35.7, 28.7, 28.3, 28.2, 28.2, 26.8; HRMS (ESI-TOF) m/z: $[M + Na]^+$ calcd for $C_{28}H_{37}NO_8Na$, 538.2417; found, 538.2415.

***Tert*-butyl (E)-3-(2-(2-(Tert-butoxy)-2-oxoethyl)-6-(3-(Tert-butoxy)-3-oxopropyl)-1,3-dioxoisoindolin-5-yl)acrylate (5).**

https://dx.doi.org/10.1021/acs.joc.0c02401
J. Org. Chem. 2021, 86, 1549−1559

Compounds **5** and **6** were isolated by silica gel chromatography (hexane/ethyl acetate = 6:1) to give a mixture (with a molar ratio of roughly 0.7:1 as estimated from ^{1}H NMR analysis) as a yellow solid (32 mg, 12%) from the synthesis procedure of **EDY-A** in which the reaction system was further heated to 50 °C in an oil bath for a week. ^{1}H NMR (600 MHz, $CDCl_3$): δ 8.01 (s, 1H), 7.90 (d, J = 15.7 Hz, 1H), 7.75 (s, 1H), 6.45 (d, J = 15.7 Hz, 1H), 4.32 (s, 2H), 3.15 (t, J = 7.6 Hz, 2H), 2.56 (t, J = 7.6 Hz, 2H), 1.54 (s, 9H), 1.45 (s, 9H), 1.42 (s, 9H); ^{13}C{^{1}H} NMR (151 MHz, CD_3OD): δ 171.0, 167.1, 166.4, 166.2, 165.3, 146.8, 139.6, 138.6, 132.3, 130.6, 125.8, 124.8, 121.8, 82.9, 81.8, 81.1, 39.8, 35.7, 28.7, 28.1, 28.0, 28.0; HRMS (ESI-TOF) m/z: [M + Na]$^+$ calcd for $C_{28}H_{37}NO_8Na$, 538.2417; found, 538.2418.

***Tert*-butyl 2-(2-(Tert-butoxy)-2-oxoethyl)-7-(3-(tert-butoxy)-3-oxopropyl)-1,3-dioxo-2,3,6,7-tetrahydro-1*H*-cyclobuta[*e*]isoindole-6-carboxylate (6).** ^{1}H NMR (600 MHz, $CDCl_3$): δ 7.80 (d, J = 7.5 Hz, 1H), 7.47 (dd, J = 7.5, 1.1 Hz, 1H), 4.34−4.26 (m, 2H), 4.01 (dd, J = 2.8, 1.1 Hz, 1H), 3.93 (ddd, J = 9.0, 6.6, 2.8 Hz, 1H), 2.66−2.51 (m, 2H), 2.33−2.28 (m, 1H), 2.14−2.08 (m, 1H), 1.47 (s, 9H), 1.46 (s, 9H), 1.45 (s, 9H); ^{13}C{^{1}H} NMR (151 MHz, $CDCl_3$): δ 172.3, 169.4, 169.4, 167.8, 166.3, 148.9, 144.8, 132.2, 127.5, 126.5, 123.8, 82.8, 81.3, 80.4, 54.2, 48.3, 39.6, 33.6, 28.3, 28.1, 28.0, 28.0; HRMS (ESI-TOF) m/z: [M + Na]$^+$ calcd for $C_{28}H_{37}NO_8Na$, 538.2417; found, 538.2418.

3-(4-Iodo-1-neopentyl-2,5-dioxo-2,5-dihydro-1*H*-pyrrol-3-yl)prop-2-yn-1-yl Acetate (3S). The compound **3S** was synthesized by Sonogashira coupling between compound **2S**[29] and **2**. The mixture was stirred at ambient temperature until completion of the reaction as detected by TLC (13 h). After that, the mixture was subjected to silica gel chromatography (hexane/ethyl acetate = 10:1) to give a yellow oil (35 mg, 18%). ^{1}H NMR (600 MHz, $CDCl_3$): δ 4.94 (s, 2H), 3.39 (s, 2H), 2.14 (s, 3H), 0.91 (s, 9H); ^{13}C{^{1}H} NMR (151 MHz, $CDCl_3$): δ 170.2, 167.1, 166.9, 135.9, 108.9, 102.6, 77.6, 52.6, 51.1, 33.8, 28.0, 20.8; HRMS (ESI-TOF) m/z: [M + Na]$^+$ calcd for $C_{14}H_{16}INO_4Na$, 412.0022; found, 412.0023.

Di*tert*-butyl 5,5′-(1-benzyl-2,5-dioxo-2,5-dihydro-1*H*-pyrrole-3,4-diyl)bis(pent-4-ynoate) (EDY-C). The **EDY-C** was synthesized by Sonogashira coupling between compound **4S**[13] and **1**. The mixture was stirred at ambient temperature until completion of the reaction as detected by TLC (6 h). After that, the mixture was subjected to silica gel chromatography (hexane/ethyl acetate = 6:1) to give a yellow oil (147 mg, 60%). ^{1}H NMR (600 MHz, $CDCl_3$): δ 7.34−7.25 (m, 5H), 4.66 (s, 2H), 2.81 (t, J = 7.5 Hz, 4H), 2.57 (t, J = 7.5 Hz, 4H), 1.46 (s, 18H); ^{13}C{^{1}H} NMR (151 MHz, $CDCl_3$): δ 170.6, 167.1, 135.9, 128.8, 128.7, 128.4, 128.1, 110.0, 81.2, 71.9, 42.4, 34.0, 28.2, 16.6; HRMS (ESI-TOF) m/z: [M + Na]$^+$ calcd for $C_{29}H_{33}NO_6Na$, 514.2206; found, 514.2205.

■ ASSOCIATED CONTENT

Supporting Information

The Supporting Information is available free of charge at https://pubs.acs.org/doi/10.1021/acs.joc.0c02401.

Experimental procedure and fundamental characterization (PDF)

■ AUTHOR INFORMATION

Corresponding Authors

Yun Ding − *Shanghai Key Laboratory of Advanced Polymeric Materials, School of Materials Science and Engineering, East China University of Science and Technology, Shanghai 200237, China;* orcid.org/0000-0002-7012-5621; Email: yunding@ecust.edu.cn

Aiguo Hu − *Shanghai Key Laboratory of Advanced Polymeric Materials, School of Materials Science and Engineering, East China University of Science and Technology, Shanghai 200237, China;* orcid.org/0000-0003-0456-7269; Email: hagmhsn@ecust.edu.cn

Authors

Mengsi Zhang − *Shanghai Key Laboratory of Advanced Polymeric Materials, School of Materials Science and Engineering, East China University of Science and Technology, Shanghai 200237, China*

Haotian Lu − *Shanghai Key Laboratory of Advanced Polymeric Materials, School of Materials Science and Engineering, East China University of Science and Technology, Shanghai 200237, China*

Baojun Li − *Shanghai Key Laboratory of Advanced Polymeric Materials, School of Materials Science and Engineering, East China University of Science and Technology, Shanghai 200237, China*

Hailong Ma − *Shanghai Key Laboratory of Advanced Polymeric Materials, School of Materials Science and Engineering, East China University of Science and Technology, Shanghai 200237, China*

Wenbo Wang − *Shanghai Key Laboratory of Advanced Polymeric Materials, School of Materials Science and Engineering, East China University of Science and Technology, Shanghai 200237, China*

Xiaoyu Cheng − *Shanghai Key Laboratory of Advanced Polymeric Materials, School of Materials Science and Engineering, East China University of Science and Technology, Shanghai 200237, China*

Complete contact information is available at: https://pubs.acs.org/10.1021/acs.joc.0c02401

Author Contributions

This article was written through contributions of all authors.

Notes

The authors declare no competing financial interest.

■ ACKNOWLEDGMENTS

Dedicated to the 100th anniversary of Chemistry at Nankai University. The authors gratefully acknowledge the financial support from the National Natural Science Foundation of China (21871080 and 21503078), the Fundamental Research Funds for the Central Universities (22221818014), and Shanghai Leading Academic Discipline Project (B502). A.H. thanks the "Eastern Scholar Professorship" support from Shanghai local government.

■ REFERENCES

(1) Romeo, R.; Giofre, S. V.; Chiacchio, M. A. Synthesis and Biological Activity of Unnatural Enediynes. *Curr. Med. Chem.* **2017**, *24*, 3433−3484.

(2) Grdičak, M.; Jerić, I. Enediyne compounds-new promises in anticancer therapy. *Acta Pharm.* **2007**, *57*, 133−150.

(3) Mohamed, R. K.; Peterson, P. W.; Alabugin, I. V. Concerted Reactions That Produce Diradicals and Zwitterions: Electronic, Steric, Conformational, and Kinetic Control of Cycloaromatization Processes. *Chem. Rev.* **2013**, *113*, 7089−7129.

(4) Jones, R. R.; Bergman, R. G. p-Benzyne. Generation as an intermediate in a thermal isomerization reaction and trapping evidence for the 1,4-benzenediyl structure. *J. Am. Chem. Soc.* **1972**, *94*, 660−661.

(5) Bergman, R. G. Reactive 1,4-Dehydroaromatics. *Acc. Chem. Res.* **1973**, *6*, 25−31.

(6) Lockhart, T. P.; Comita, P. B.; Bergman, R. G. Kinetic evidence for the formation of discrete 1,4-dehydrobenzene intermediates. Trapping by inter- and intramolecular hydrogen atom transfer and observation of high-temperature CIDNP. *J. Am. Chem. Soc.* **1981**, *103*, 4082−4090.

(7) Roy, S. K.; Basak, A. Synthesis and reactivity of a 9-membered azaenediyne: importance of proximity effect in N-alkylation. *Chem. Commun.* **2006**, 1646−1648.
(8) Godwin, C. D.; Gale, R. P.; Walter, R. B. Gemtuzumab ozogamicin in acute myeloid leukemia. *Leukemia* **2017**, *31*, 1855−1868.
(9) Hamann, P. R.; Hinman, L. M.; Beyer, C. F.; Lindh, D.; Upeslacis, J.; Flowers, D. A.; Bernstein, I. An Anti-CD33 Antibody-Calicheamicin Conjugate for Treatment of Acute Myeloid Leukemia. Choice of Linker. *Bioconjugate Chem.* **2002**, *13*, 40−46.
(10) Nicolaou, K. C.; Das, D.; Lu, Y.; Rout, S.; Pitsinos, E. N.; Lyssikatos, J.; Schammel, A.; Sandoval, J.; Hammond, M.; Aujay, M.; Gavrilyuk, J. Total Synthesis and Biological Evaluation of Tiancimycins A and B, Yangpumicin A, and Related Anthraquinone-Fused Enediyne Antitumor Antibiotics. *J. Am. Chem. Soc.* **2020**, *142*, 2549−2561.
(11) Nicolaou, K. C.; Wang, Y.; Lu, M.; Mandal, D.; Pattanayak, M. R.; Yu, R.; Shah, A. A.; Chen, J. S.; Zhang, H.; Crawford, J. J.; Pasunoori, L.; Poudel, Y. B.; Chowdari, N. S.; Pan, C.; Nazeer, A.; Gangwar, S.; Vite, G.; Pitsinos, E. N. Streamlined Total Synthesis of Uncialamycin and Its Application to the Synthesis of Designed Analogues for Biological Investigations. *J. Am. Chem. Soc.* **2016**, *138*, 8235−8246.
(12) Nicolaou, K. C.; Lu, Z.; Li, R.; Woods, J. R.; Sohn, T.-i. Total Synthesis of Shishijimicin A. *J. Am. Chem. Soc.* **2015**, *137*, 8716−8719.
(13) Li, B.; Zhang, M.; Lu, H.; Ma, H.; Wang, Y.; Chen, H.; Ding, Y.; Hu, A. Coordination-Accelerated Radical Formation from Acyclic Enediynes for Tumor Cell Suppression. *Chem. Asian J.* **2019**, *14*, 4352−4357.
(14) Li, B.; Duan, B.; Li, J.; Zhang, M.; Yuan, Y.; Ding, Y.; Hu, A. An Acyclic Enediyne Anticancer Compound Attributed to a Bergman Cyclization at Physiological Temperature. *Tetrahedron* **2018**, *74*, 6419−6425.
(15) Joshi, M. C.; Rawat, D. S. Recent Developments in Enediyne Chemistry. *Chem. Biodiversity* **2012**, *9*, 459−498.
(16) Kar, M.; Basak, A. Design, Synthesis, and Biological Activity of Unnatural Enediynes and Related Analogues Equipped with pH-Dependent or Phototriggering Devices. *Chem. Rev.* **2007**, *107*, 2861−2890.
(17) Karpov, G.; Kuzmin, A.; Popik, V. V. Enhancement of the Reactivity of Photochemically Generated Enediynes via Keto−Enol Tautomerization. *J. Am. Chem. Soc.* **2008**, *130*, 11771−11777.
(18) Banfi, L.; Guanti, G.; Rasparini, M. Intramolecular Opening of β-Lactams with Amines as a Strategy Toward Enzymatically or Photochemically Triggered Activation of Lactenediyne Prodrugs. *Eur. J. Org. Chem.* **2003**, *2003*, 1319−1336.
(19) Pandithavidana, D. R.; Poloukhtine, A.; Popik, V. V. Photochemical Generation and Reversible Cycloaromatization of a Nine-Membered Ring Cyclic Enediyne. *J. Am. Chem. Soc.* **2009**, *131*, 351−356.
(20) Myers, A. G.; Dragovich, P. S.; Kuo, E. Y. Studies on the thermal generation and reactivity of a class of (.sigma.,.pi.)-1,4-biradicals. *J. Am. Chem. Soc.* **1992**, *114*, 9369−9386.
(21) Nagata, R.; Yamanaka, H.; Murahashi, E.; Saito, I. DNA cleavage by acyclic eneyne-allene systems related to neocarzinostatin and esperamicin-calicheamicin. *Tetrahedron Lett.* **1990**, *31*, 2907−2910.
(22) Myers, A. G.; Cohen, S. B.; Kwon, B.-M.B. DNA cleavage by neocarzinostatin chromophore. Establishing the intermediacy of chromophore-derived cumulene and biradical species and their role in sequence-specific cleavage. *J. Am. Chem. Soc.* **1994**, *116*, 1670−1682.
(23) Suzuki, I.; Naoe, Y.; Bando, M.; Nemoto, H.; Shibuya, M. pH Dependent cycloaromatization of enediyne model compounds via γ-oxo ketene acetal intermediates. *Tetrahedron Lett.* **1998**, *39*, 2361−2364.
(24) Toshima, K.; Ohta, K.; Ohashi, A.; Nakamura, T.; Nakata, M.; Tatsuta, K.; Matsumura, S. Molecular Design, Chemical Synthesis, and Study of Novel Enediyne-Sulfide Systems Related to the Neocarzinostatin Chromophore. *J. Am. Chem. Soc.* **1995**, *117*, 4822−4831.
(25) Zhao, J.; Hughes, C. O.; Toste, F. D. Synthesis of Aromatic Ketones by a Transition Metal-Catalyzed Tandem Sequence. *J. Am. Chem. Soc.* **2006**, *128*, 7436−7437.
(26) Raviola, C.; Protti, S.; Ravelli, D.; Fagnoni, M. (Hetero)-aromatics from dienynes, enediynes and enyne-allenes. *Chem. Soc. Rev.* **2016**, *45*, 4364−4390.
(27) dos Passos Gomes, G.; Morrison, A. E.; Dudley, G. B.; Alabugin, I. V. Optimizing Amine-Mediated Alkyne−Allene Isomerization to Improve Benzannulation Cascades: Synergy between Theory and Experiments. *Eur. J. Org. Chem.* **2019**, *2019*, 512−518.
(28) Martinez-Erro, S.; Sanz-Marco, A.; Bermejo Gómez, A.; Vázquez-Romero, A.; Ahlquist, M. S. G.; Martín-Matute, B. Base-Catalyzed Stereospecific Isomerization of Electron-Deficient Allylic Alcohols and Ethers through Ion-Pairing. *J. Am. Chem. Soc.* **2016**, *138*, 13408−13414.
(29) Zhang, M.; Li, B.; Chen, H.; Lu, H.; Ma, H.; Cheng, X.; Wang, W.; Wang, Y.; Ding, Y.; Hu, A. Triggering the Antitumor Activity of Acyclic Enediyne through Maleimide-Assisted Rearrangement and Cycloaromatization. *J. Org. Chem.* **2020**, *85*, 9808−9819.
(30) Andemichael, Y. W.; Gu, Y. G.; Wang, K. K. Stereoselective synthesis of both (E)- and (Z)-1,2,4-heptatrien-6-ynes. Formation of an .alpha.,3-dehydrotoluene biradical, trapping by an intramolecular carbon-carbon double bond, and decay of the resulting new biradical via an intramolecular route. *J. Org. Chem.* **1992**, *57*, 794−796.
(31) Andemichael, Y. W.; Huang, Y.; Wang, K. K. Thermally-induced one-step construction of the tetracyclic steroidal skeleton from acyclic enyne-allenes. *J. Org. Chem.* **1993**, *58*, 1651−1652.
(32) Gaudel-Siri, A.; Campolo, D.; Mondal, S.; Nechab, M.; Siri, D.; Bertrand, M. P. Theoretical study to explain how chirality is stored and evolves throughout the radical cascade rearrangement of enyne-allenes. *J. Org. Chem.* **2014**, *79*, 9086−9093.
(33) Campolo, D.; Gaudel-Siri, A.; Mondal, S.; Siri, D.; Besson, E.; Vanthuyne, N.; Nechab, M.; Bertrand, M. P. Mechanistic Investigation of Enediyne-Connected Amino Ester Rearrangement. Theoretical Rationale for the Exclusive Preference for 1,6- or 1,5-Hydrogen Atom Transfer Depending on the Substrate. A Potential Route to Chiral Naphthoazepines. *J. Org. Chem.* **2012**, *77*, 2773−2783.
(34) Baroudi, A.; Mauldin, J.; Alabugin, I. V. Conformationally Gated Fragmentations and Rearrangements Promoted by Interception of the Bergman Cyclization through Intramolecular H-Abstraction: A Possible Mechanism of Auto-Resistance to Natural Enediyne Antibiotics? *J. Am. Chem. Soc.* **2010**, *132*, 967−979.
(35) Song, D.; Sun, S.; Tian, Y.; Huang, S.; Ding, Y.; Yuan, Y.; Hu, A. Maleimide-Based Acyclic Enediyne for Efficient DNA-Cleavage and Tumor Cell Suppression. *J. Mater. Chem. B* **2015**, *3*, 3195−3200.
(36) Lu, H.; Ma, H.; Li, B.; Zhang, M.; Chen, H.; Wang, Y.; Li, X.; Ding, Y.; Hu, A. Facilitating Myers-Saito cyclization through acid-triggered tautomerization for the development of maleimide-based antitumor agents. *J. Mater. Chem. B* **2020**, *8*, 1971−1979.
(37) Wang, Y.; Li, B.; Zhang, M.; Lu, H.; Chen, H.; Wang, W.; Ding, Y.; Hu, A. Preparation and antitumor applications of asymmetric propargyl amide maleimide based enediyne antibiotics. *Tetrahedron* **2020**, *76*, 131242.
(38) Chen, H.; Li, B.; Zhang, M.; Lu, H.; Wang, Y.; Wang, W.; Ding, Y.; Hu, A. Preparation of Maleimide-Based Enediynes with Propargyl Ester for Efficient Tumor Cell Suppression. *ChemistrySelect* **2020**, *5*, 7069−7075.
(39) Zhou, H.; Xing, Y.; Yao, J.; Lu, Y. Heteroatom as a Promotor: Synthesis of Polyfunctionalized Benzenes and Naphthalenes. *J. Org. Chem.* **2011**, *76*, 4582−4590.
(40) Beauchard, A.; Phillips, V. A.; Lloyd, M. D.; Threadgill, M. D. Synthesis of 2-(4-carboxybutenyl)- and 2-(4-carboxybutynyl)-cyclopentene-1-carboxamides. *Tetrahedron* **2009**, *65*, 8176−8184.
(41) Li, B.; Wu, Y.; Wang, Y.; Zhang, M.; Chen, H.; Li, J.; Liu, R.; Ding, Y.; Hu, A. Light-Cross-linked Enediyne Small-Molecule

https://dx.doi.org/10.1021/acs.joc.0c02401
J. Org. Chem. 2021, 86, 1549−1559

Micelle-Based Drug-Delivery System. *ACS Appl. Mater. Interfaces* **2019**, *11*, 8896−8903.
(42) Fisher, T. J.; Dussault, P. H. Regioselective Synthesis of Tetraalkynylarenes by Consecutive Dual Sonogashira Coupling Reactions of the Bis(triflate) of 4,5-Diiodobenzene-1,2-diol. *Eur. J. Org. Chem.* **2012**, *2012*, 2831−2836.
(43) Sharma, M.; Joshi, M. C.; Kumar, V.; Malhotra, S. V.; Rawat, D. S. Synthesis and Anticancer Activity of 13-Membered Cyclic Enediynes. *Arch. Pharm.* **2011**, *344*, 564−571.
(44) Ghosh, D.; Basu, S.; Singha, M.; Das, J.; Bhattacharya, P.; Basak, A. Synthesis of crescent shaped heterocycle-fused aromatics via Garratt-Braverman cyclization and their DNA-binding studies. *Tetrahedron Lett.* **2017**, *58*, 2014−2018.
(45) Alonso-Marañón, L.; Sarandeses, L. A.; Martínez, M. M.; Pérez Sestelo, J. Synthesis of fused chromenes by the indium(iii)-catalyzed cascade hydroarylation/cycloisomerization reactions of polyyne-type aryl propargyl ethers. *Org. Chem. Front.* **2018**, *5*, 2308−2312.
(46) Miao, C.; Zhi, J.; Sun, S.; Yang, X.; Hu, A. Formation of Conjugated Polynaphthalene via Bergman Cyclization. *J. Polym. Sci., Polym. Chem. Ed.* **2010**, *48*, 2187−2193.
(47) Zeidan, T. A.; Kovalenko, S. V.; Manoharan, M.; Alabugin, I. V. Ortho effect in the Bergman cyclization: Comparison of experimental approaches and dissection of cycloaromatization kinetics. *J. Org. Chem.* **2006**, *71*, 962−975.
(48) Danilkina, N. A.; Kulyashova, A. E.; Khlebnikov, A. F.; Bräse, S.; Balova, I. A. Electrophilic Cyclization of Aryldiacetylenes in the Synthesis of Functionalized Enediynes Fused to a Heterocyclic Core. *J. Org. Chem.* **2014**, *79*, 9018−9045.
(49) Alabugin, I. V.; Manoharan, M. Reactant Destabilization in the Bergman Cyclization and Rational Design of Light- and pH-Activated Enediynes. *J. Phys. Chem. A* **2003**, *107*, 3363−3371.
(50) Hohenberg, P.; Kohn, W. Inhomogeneous Electron Gas. *Phys. Rev. B: Condens. Matter Mater. Phys.* **1964**, *136*, 864−871.
(51) Kohn, W.; Sham, L. J. Self-Consistent Equations Including Exchange and Correlation Effects. *Phys. Rev.* **1965**, *140*, A1133−A1138.
(52) Janzen, E. G.; Blackburn, B. J. Detection and identification of short-lived free radicals by an electron spin resonance trapping technique. *J. Am. Chem. Soc.* **1968**, *90*, 5909−5910.
(53) Zeidan, T. A.; Manoharan, M.; Alabugin, I. V. Ortho effect in the Bergman cyclization: Interception of p-benzyne intermediate by intramolecular hydrogen abstraction. *J. Org. Chem.* **2006**, *71*, 954−961.
(54) Iida, K.-i.; Hirama, M. Synthesis and Characterization of Nine-Membered Cyclic Enediynes, Models of the C-1027 and Kedarcidin Chromophores: Equilibration with a p-Benzyne Biradical and Kinetic Stabilization. *J. Am. Chem. Soc.* **1995**, *117*, 8875−8876.
(55) Usuki, T.; Nakanishi, K.; Ellestad, G. A. Spin-trapping of the p-benzyne intermediates from ten-membered enediyne calicheamicin gamma1I. *Org. Lett.* **2006**, *8*, 5461−5463.
(56) Usuki, T.; Kawai, M.; Nakanishi, K.; Ellestad, G. A. Calicheamicin gamma(I)(1) and phenyl tert-butyl nitrone (PBN): observation of a kinetic isotope effect by an ESR study. *Chem. Commun.* **2010**, *46*, 737−739.
(57) Grissom, J. W.; Klingberg, D.; Huang, D.; Slattery, B. J. Tandem Enyne Allene-Radical Cyclization: Low-Temperature Approaches to Benz[e]indene and Indene Compounds. *J. Org. Chem.* **1997**, *62*, 603−626.
(58) Vavilala, C.; Byrne, N.; Kraml, C. M.; Ho, D. M.; Pascal, R. A. Thermal C1-C5 Diradical Cyclization of Enediynes. *J. Am. Chem. Soc.* **2008**, *130*, 13549−13551.
(59) Oguadinma, P.; Bilodeau, F.; LaPlante, S. R. NMR strategies to support medicinal chemistry workflows for primary structure determination. *Bioorg. Med. Chem. Lett.* **2017**, *27*, 242−247.
(60) Davenport, R.; Silvi, M.; Noble, A.; Hosni, Z.; Fey, N.; Aggarwal, V. K. Visible-Light-Driven Strain-Increase Ring Contraction Allows the Synthesis of Cyclobutyl Boronic Esters. *Angew. Chem., Int. Ed.* **2020**, *59*, 6525−6528.
(61) Frisch, M. J.; Trucks, G. W.; Schlegel, H. B.; Scuseria, G. E.; Robb, M. A.; Cheeseman, J. R.; Scalmani, G.; Barone, V.; Mennucci, B.; Petersson, G. A.; Nakatsuji, H.; Caricato, M.; Li, X.; Hratchian, H. P.; Izmaylov, A. F.; Bloino, J.; Zheng, G.; Sonnenberg, J. L.; Hada, M.; Ehara, M.; Toyota, K.; Fukuda, R.; Hasegawa, J.; Ishida, M.; Nakajima, T.; Honda, Y.; Kitao, O.; Nakai, H.; Vreven, T.; Montgomery, J. A., Jr.; Peralta, J. E.; Ogliaro, F.; Bearpark, M.; Heyd, J. J.; Brothers, E.; Kudin, K. N.; Staroverov, V. N.; Kobayashi, R.; Normand, J.; Raghavachari, K.; Rendell, A.; Burant, J. C.; Iyengar, S. S.; Tomasi, J.; Cossi, M.; Rega, N.; Millam, J. M.; Klene, M.; Knox, J. E.; Cross, J. B.; Bakken, V.; Adamo, C.; Jaramillo, J.; Gomperts, R.; Stratmann, R. E.; Yazyev, O.; Austin, A. J.; Cammi, R.; Pomelli, C.; Ochterski, J. W.; Martin, R. L.; Morokuma, K.; Zakrzewski, V. G.; Voth, G. A.; Salvador, P.; Dannenberg, J. J.; Dapprich, S.; Daniels, A. D.; Farkas, Ö.; Foresman, J. B.; Ortiz, J. V.; Cioslowski, J.; Fox, D. J.; Gaussian, Inc.: Wallingford CT, 2009.
(62) Cossi, M.; Scalmani, G.; Rega, N.; Barone, V. New developments in the polarizable continuum model for quantum mechanical and classical calculations on molecules in solution. *J. Chem. Phys.* **2002**, *117*, 43−54.
(63) Wong, M. W.; Wiberg, K. B.; Frisch, M. J. Solvent effects. 3. Tautomeric equilibria of formamide and 2-pyridone in the gas phase and solution: an ab initio SCRF study. *J. Am. Chem. Soc.* **1992**, *114*, 1645−1652.
(64) Yuan, B.; He, R.; Shen, W.; Li, M. Influence of Base Strength on the Proton-Transfer Reaction by Density Functional Theory. *Eur. J. Org. Chem.* **2017**, *2017*, 3947−3956.
(65) Poutsma, M. L. Evaluation of the Kinetic Data for Intramolecular 1,x-Hydrogen Shifts in Alkyl Radicals and Structure/Reactivity Predictions from the Carbocyclic Model for the Transition State. *J. Org. Chem.* **2007**, *72*, 150−161.
(66) Schöneich, C.; Mozziconacci, O.; Koppenol, W. H.; Nauser, T. Intramolecular 1,2- and 1,3-Hydrogen Transfer Reactions of Thiyl Radicals. *Isr. J. Chem.* **2014**, *54*, 265−271.
(67) da Silva, G.; Kim, C.-H.; Bozzelli, J. W. Thermodynamic Properties (Enthalpy, Bond Energy, Entropy, and Heat Capacity) and Internal Rotor Potentials of Vinyl Alcohol, Methyl Vinyl Ether, and Their Corresponding Radicals. *J. Phys. Chem. A* **2006**, *110*, 7925−7934.
(68) Hu, X.; Li, H.; Liang, W.; Han, S. Systematic Study of the Tautomerism of Uracil Induced by Proton Transfer. Exploration of Water Stabilization and Mutagenicity. *J. Phys. Chem. B* **2005**, *109*, 5935−5944.
(69) Bhattacharya, P.; Singha, M.; Das, E.; Mandal, A.; Maji, M.; Basak, A. Recent advances in Garratt-Braverman cyclization: Mechanistic and synthetic explorations. *Tetrahedron Lett.* **2018**, *59*, 3033−3051.
(70) Alcaide, B.; Almendros, P.; Aragoncillo, C. Exploiting [2+2] cycloaddition chemistry: achievements with allenes. *Chem. Soc. Rev.* **2010**, *39*, 783−816.

https://dx.doi.org/10.1021/acs.joc.0c02401
J. Org. Chem. 2021, 86, 1549−1559